

HIGHER TEMPERATURES GENERICALLY FAVOR SLOWER-GROWING BACTERIAL SPECIES IN MULTISPECIES COMMUNITIES

Simon Lax, Clare I. Abreu, & Jeff Gore

Department of Physics, Massachusetts Institute of Technology, Cambridge, MA, USA

Correspondence to S.L. (simonlax@mit.edu) and J.G. (gore@mit.edu)

1 Temperature is among the cardinal environmental variables which determine the
2 composition and function of microbial communities. Many culture-independent studies have
3 characterized communities that are affected by changing temperatures, either due to seasonal
4 cycles¹⁻³, long-term warming⁴⁻⁶, or latitudinal/elevational gradients⁷⁻⁸. However, a predictive
5 understanding of how microbial communities respond to such changes in temperature is still
6 lacking, partly because it is not obvious which aspects of microbial physiology determine whether
7 a species should benefit from temperature alteration. Here, we incorporate how microbial growth
8 rates change with temperature to a modified Lotka-Volterra competition model⁹, and predict that
9 higher temperatures should generically favor slower-growing species in a bacterial community. We
10 experimentally confirm this prediction in pairwise cocultures assembled from a diverse set of
11 species, and we show that these changes to pairwise outcomes with temperature are also predictive
12 of changing outcomes in three-species communities, suggesting our theory may propagate to more
13 complex assemblages. Our results demonstrate that it is possible to predict how bacterial
14 communities will shift with temperature knowing only the growth rates of the community members.
15 These results provide a testable hypothesis for future studies of more complex, natural
16 communities, and we hope that this work will help bridge the gap between ecological theory and
17 the complex dynamics observed in metagenomic surveys.

18 Experimental microbial communities are normally incubated at a fixed temperature. We aimed to
19 determine how changing this incubation temperature would affect the outcome of a microbial coculture in
20 which the two species were known to stably coexist at our usual experimental temperature of 25°C. We
21 focused on two naturally co-occurring species isolated from soil (Aci1 and Pan1), and followed a standard
22 coculture methodology (see Methods) at three experimental temperatures: 16°C, 25°C, and 30°C. At each
23 of these three temperatures, Aci1 is the faster growing species, and the difference in the growth rates of the
24 two species increases alongside temperature (**Figure 1A**). Accordingly, we assumed that the slower-growing
25 Pan1 would be favored by lowering the temperature and disfavored by raising the temperature, as its
26 competitive ability would likely be hindered by a larger disparity in growth rate. Surprisingly, we observed
27 the opposite, and found that Pan1 in fact becomes a *stronger* competitor at higher temperature, with the
28 coculture outcome shifting from Aci1 dominance at 16°C (**Figure 1B**) to coexistence at 25°C (**Figure 1C**)
29 and finally to Pan1 dominance at 30°C (**Figure 1D**).

30 To explain this potentially counterintuitive result, we developed a model that expands on the work
31 of Abreu *et al.*⁹, who used a modified version of the Lotka-Volterra competition model to explain how
32 increasing mortality favors faster growing species. In addition to the growth rates, the Lotka-Volterra model
33 requires knowledge of how the growth of the two species is inhibited by other cells of their own species as
34 compared to the presence of cells of the competing species. This inhibition is traditionally captured by a
35 parameter (α) that relates the strength of interspecific (between-species) competition to intraspecific (within-
36 species) competition (**Figure 2A**). Competitive outcomes in the classic version of this model are determined
37 entirely by these competition coefficients. However, many microbial communities experience mortality that
38 is not driven by competition and which affects the entire community. Importantly, this is true of all
39 laboratory cultures, where cells are removed from the community either continuously (as in a chemostat or
40 turbidostat) or at discrete intervals (as in batch culture). It may also result from predation by bacterivores,
41 or from physical removal, as in our gut microbiota. The formulation of the Lotka-Volterra model described
42 above can therefore be made more realistic to microbial cocultures by the introduction of a community-
43 wide mortality rate (δ). The introduction of this death rate to the model (**Figure 2B**) has an important effect:
44 it makes the competitive outcome dependent on the growth rates as well as the competition coefficients,
45 such that when the death rate is absorbed the α 's are reparametrized as

$$\hat{\alpha}_{ij} = \alpha_{ij} \frac{1 - \frac{\delta}{r_j}}{1 - \frac{\delta}{r_i}}$$

46 where α_{ij} is the inhibition of species i by species j without the death rate and $\hat{\alpha}_{ij}$ is the inhibition with the
47 death rate. Adding mortality to the model favors the faster growing species⁹ by increasing α_{sf} and decreasing
48 α_{fs} . Visually, this change to the α 's of the two species can be represented as a 45-degree arrow through the
49 phase space of the competitive outcomes (**Figure 2C**), pointing to the quadrant in which the faster grower
50 wins. Mortality can reverse the competitive outcome if the slow grower would win without the mortality
51 rate, passing first through a region of either coexistence or bistability. Importantly, the arrow is made longer
52 by higher death rates and made shorter by higher growth rates. As bacterial growth rates are a function of
53 temperature, this in turn introduces a temperature-dependence to the competition, and suggests that at any
54 given death rate higher temperature should favor the slower growing species by lessening the favor conferred
55 to the fast grower by the added mortality.

56 To understand how temperature should influence the growth rate of bacterial species, we turned to
57 the model of Ratkowsky *et al.*¹⁰. This phenomenological model predicts a linear relationship between
58 temperature and the square root of a species' growth rate, such that the growth rate of any bacterial species
59 can be modeled (so long as it is sufficiently below the species' optimum temperature, T_{Op}) as a function of
60 two parameters: the slope of the presumed linear relationship (b), and the x-intercept of that line ($T0$) (**Figure**

61 **2D**). For any pair of species in which there is a consistent fast-grower (i.e. the faster grower has the lower
62 T_0 and the higher b), plugging the Ratkowsky model into the competition model and taking the derivative
63 of α_{is} with respect to temperature reveals the surprising prediction that the slow grower is *always* favored by
64 an increase in temperature. Remarkably, this is true even if the difference in growth rates between the two
65 species increases with temperature. The prediction is largely generalizable to any temperature range in which
66 there is a consistent faster-growing species and slower-growing species, even if their growth rate rankings
67 flip far enough outside this temperature range (Supplementary Information). It is also generalizable to non-
68 competitive interactions such as mutualism and parasitism (Supplementary Information). There are practical
69 limits to this change to α : if the slow grower is already dominating at low temperatures then increasing
70 temperature will not lead to a qualitative change in the outcome. Additionally, this model only holds when
71 the temperature is below the species' optimums, and growth rates increase alongside increases in
72 temperature. Still, this theory suggests that it is possible to alter the competitive outcome by changing
73 temperature, and to predict which species should benefit so long as the growth rates are known.

74 As a test of this theory, we chose a collection of 13 bacterial strains with variable growth rates
75 (**Figure 3A**). This group comprised 6 strains from the ATCC culture collection and 7 naturally co-occurring
76 strains isolated from soil. To fit the Ratkowsky model, we measured the growth rates of each strain at a
77 minimum of four temperatures using a time to threshold approach (see Methods) (**Figure 3B**,
78 **Supplementary Figure 1**). Both model parameters had a wide range, with T_0 ranging from -14°C to 4°C
79 (mean = -3°C , SD = 5°C), and b ranging from 0.012 to 0.031 (mean = 0.024, SD = 0.005). Interestingly,
80 these two values were highly correlated ($\rho = 0.96$, **Supplementary Figure 2**), suggesting that species which
81 are capable of growing at lower temperatures (lower T_0), are less able to increase their growth rates as
82 temperature increases (lower b). This correlation has been previously reported in the literature¹¹, although,
83 to our knowledge, without any mechanistic explanation. It follows from the high correlation between b and
84 T_0 that the curves representing the growth rate responses to temperature of different species (**Figure 3B**)
85 are likely to intersect, such that which species we term the 'fast grower' and 'slow grower' may not be
86 consistent across our range of temperatures. However, in 39 of the possible 78 pairs of species (50%) there
87 was a consistent fast- and slow-grower across the range of experimental temperatures (16°C - 30°C) (**Figure**
88 **3C**). We carried out 38 of these 39 pairwise cocultures, but did not coculture Pan1 and Pan2 because their
89 colony morphologies are difficult to visually differentiate. For a subset of these cocultures, we varied the
90 death rate as well as the temperature to explore how these two variables interact to shape competitive
91 landscapes (Supplementary Information).

92 When these coculture outcomes are visualized as a heat map (**Figure 3D**), we observe a clear shift
93 from fast-grower dominance at 16°C towards coexistence or slow-grower dominance in most species pairs.

94 Plotting the changes in the slow-grower percentage for the two temperature shifts (**Figure 3E**) reveals that
95 almost all transitions are in keeping with our theory. Of the 73 transitions that do not include a bistable
96 outcome, 46 (63%) resulted in an increase in the slow-grower percentage in accordance with our theory, 23
97 (32%) led to no shift in the slow-grower percentage, and only 4 (5%) resulted in a decrease in the slow-
98 grower percentage counter to our theory. In two of those four pairwise transitions not predicted by the
99 model (EA/SM and Aci2/PV, both from 16°C to 25°C), the fast-grower dominated the community at 16°C
100 when its initial fraction was 90% but coexistence was observed when its initial fraction was 50% or 10%,
101 suggesting that the community may not have come to equilibrium within the 7 day experiment. In the third
102 pair's (PP/Pan2) transition from 25°C to 30°C, we always observed coexistence at both temperatures but
103 with very high variance between replicates (0.1% - 0.8% slow grower at 25°C and 0% - 0.8% slow grower at
104 30°C), suggesting either experimental error or a high degree of stochasticity in this particular interaction.
105 Finally, the fourth pair's (PCH/PV) transition from 16°C to 25°C consistently showed a switch from
106 coexistence to fast-grower dominance, suggesting some other temperature-dependent factor influenced the
107 community in a direction counter to our theory.

108 Given the success of the model in predicting pairwise outcomes, we wanted to explore how
109 temperature might impact more complex communities. Previous work in this group developed a simple
110 predictive algorithm for inferring microbial community assembly from pairwise interactions¹², which predicts
111 that any species which is outcompeted in pairwise competition will not survive in any complex community
112 that includes the other species in the pair. This implies that a change in temperature which shifts a pairwise
113 interaction from competitive exclusion to coexistence could have broad implications for other species in the
114 community, potentially resulting in cascading effects. The reverse is also possible: changes to temperature
115 might shift a competitive outcome from coexistence to exclusion, decreasing the diversity of the community
116 or allowing a species that was excluded by the newly outcompeted species to invade. We chose four trios of
117 strains to test whether the changes we observed in the pairwise dynamics propagated to a three-species
118 community. For each trio, we competed each pair of species in the trio from two initial species fractions and
119 the full trio from four initial starting fractions (**Figure 4A**). We predicted that the community assembly rules
120 should hold regardless of temperature and that increasing temperature should shift the equilibrium state
121 away from the fastest grower and towards the slowest grower (**Figure 4A**).

122 We found the community assembly rules were highly accurate: the standardized Euclidean distance
123 from the prediction had a mean of 0.11, a SD of 0.17, and was 0 in more than half of the cases (32, 52%)
124 (**Figure 4B**). Here, we focus on the PP/PCH/SM trio, in which the assembly rules predict a shift from
125 bistable dynamics between PP and PCH at low temperature, to coexistence between PCH and SM at
126 intermediate temperature, and ultimately to dominance by SM at high temperature (**Figure 4C**). In this trio,

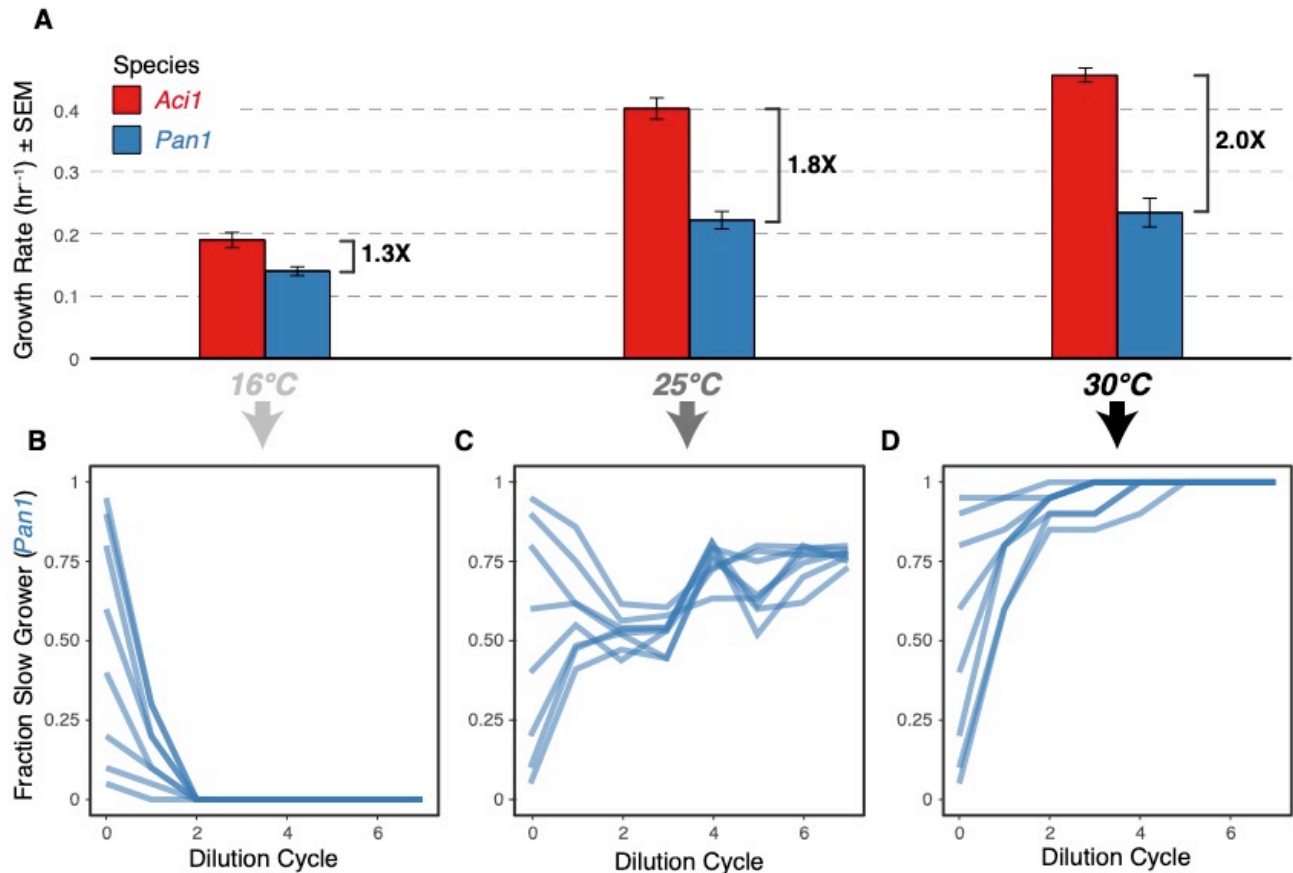
127 there is a consistent fast (PP) and slow (SM) grower across the full range of temperatures (**Figure 4D**), and
128 the predictions from the pairwise dynamics are consistent with a movement in the equilibrium species
129 fractions away from the fast grower and towards the slow grower as the temperature increases. This is in
130 fact what we observed in our experiment: in almost all cases the equilibrium result was qualitatively the same
131 as that predicted by the assembly rules. We also observed interesting dynamics in the PP/PV/Pan1 trio
132 (**Supplementary Figure 3**). Here, PV was always excluded, but the species it was excluded by changed from
133 PP to Pan1 as temperature increased. Based on the pairwise dynamics, there is possibly a temperature
134 between 25°C and 30°C where PV should have been able to persist, highlighting how even very slight
135 changes in temperature can alter the diversity of a microbial community.

136 All microbial communities are structured by interactions between their constituent species and
137 between those species and the abiotic environment. As microbes compete for space and resources they have
138 a number of tools at their disposal beyond the ability to grow faster¹³, including the production of secondary
139 metabolites that are toxic to their competitors (antibiotics), contact-dependent inhibition, or antagonistic
140 environmental alteration, for example through pH modification¹⁴. Temperature has the ability to influence
141 each of these mechanisms, for example by varying the secondary metabolites produced by the community
142 members¹⁵⁻¹⁶, manipulating the ability of community members to withstand the metabolites of other species¹⁷,
143 or changing the pH range in which a species can grow¹⁸. Temperature may also play a role in determining
144 the nutritional requirements of different species, potentially altering the nature of their ecological interactions
145 and upsetting competitive hierarchies^{19,20}. This complex set of interacting variables might suggest that
146 predicting the effect of temperature on microbial competitive outcomes requires a potentially intractable
147 knowledge of each species in the community and the interactions between them. However, we demonstrate
148 here that we can obtain a great deal of predictive accuracy knowing nothing about the mechanisms which
149 underpin those interactions and instead focusing exclusively on growth rates. This surprising simplicity may
150 result from the density dependence of each of these competitive mechanisms: the greater the gap between
151 a species' growth rate and the death rate, the more the population of that species will be able to alter the
152 environment in a manner favorable to itself. Even a very strong competitor will be rendered ineffectual if it
153 is unable to reach a sufficient density. For example, a slower-growing strain which relies on antibiotic
154 production as a competitive mechanism may not be able to produce a minimum inhibitory concentration if
155 its growth rate is barely higher than the death rate.

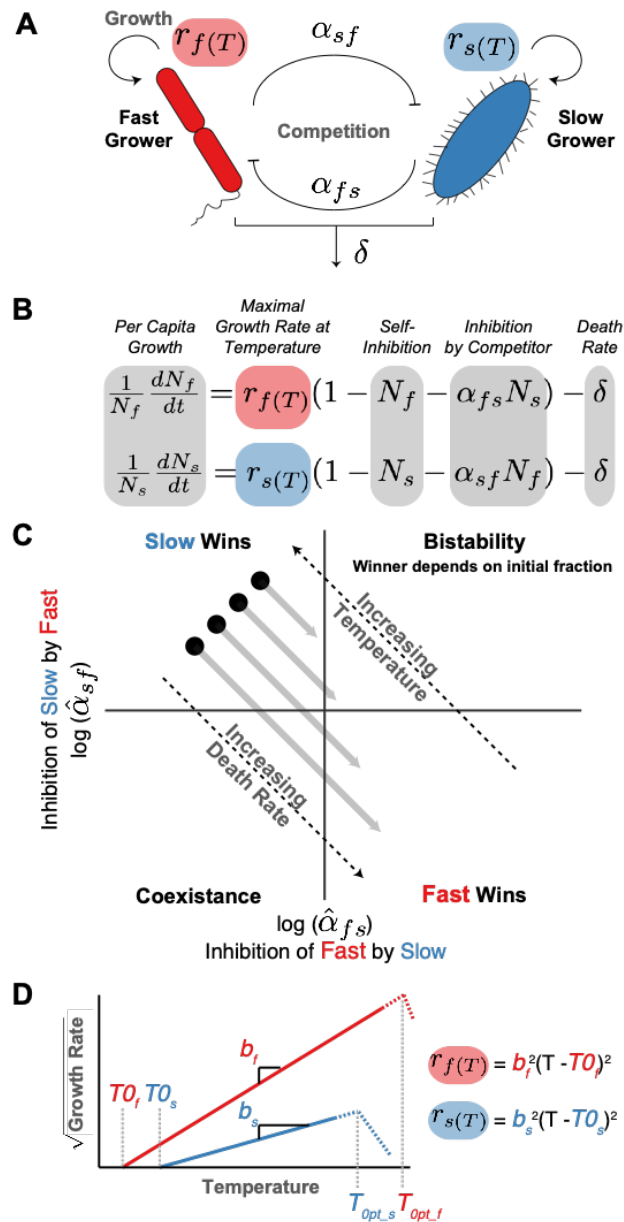
156 Here, we demonstrate a potentially unifying predictive ability that only requires knowledge of a single
157 variable: the maximal growth rate of each species. Although encouraging, these results are based on simple
158 two- or three-species communities, drawn from a small species pool, in a tightly controlled lab environment.
159 Still, this theory and preliminary experimental work provides a testable hypothesis for future studies of more

160 complex, natural communities, and helps bridge the gap between ecological theory and the complex
161 dynamics observed in metagenomic studies.

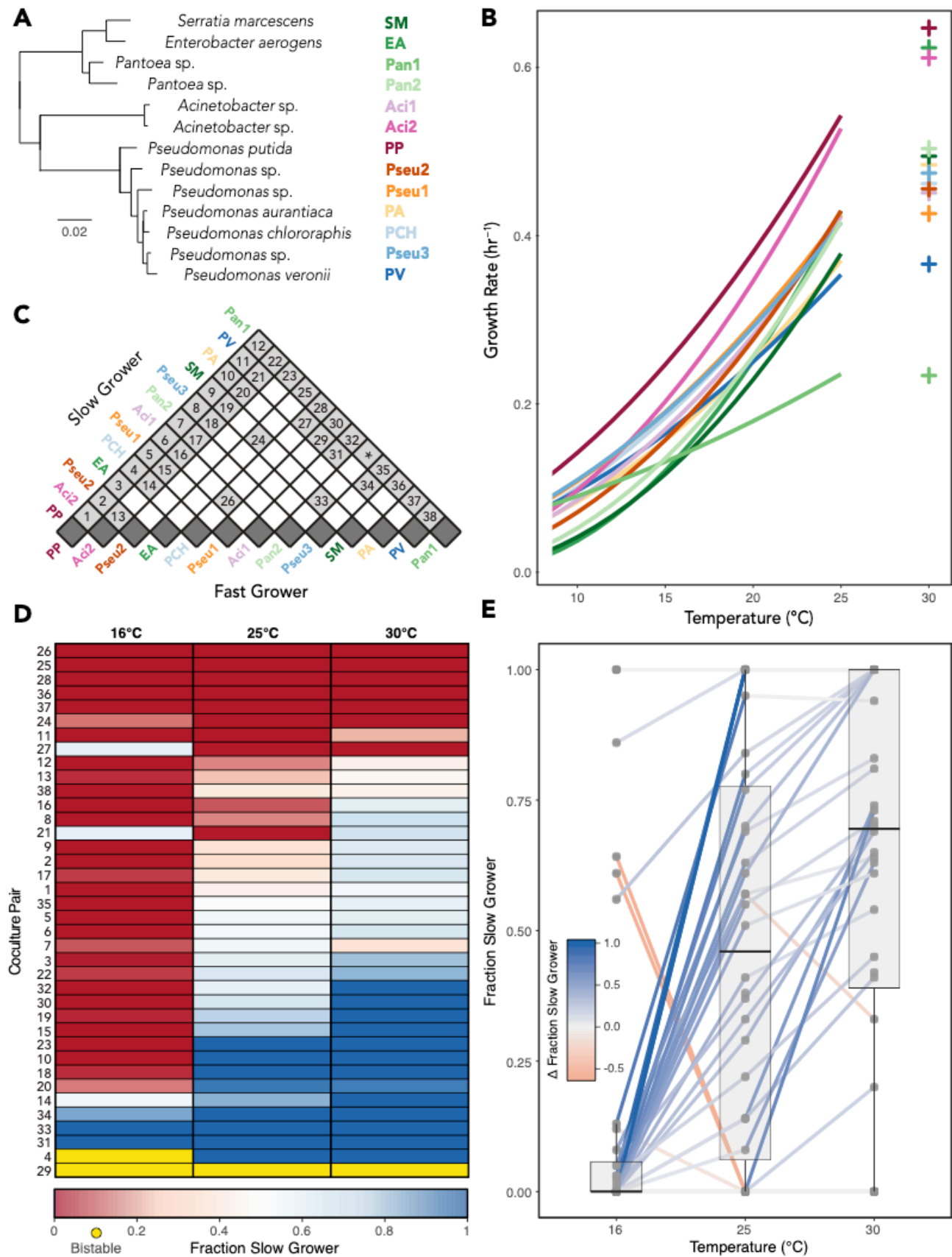
1. Gilbert, Jack A., et al. "Defining seasonal marine microbial community dynamics." *The ISME Journal* 6.2 (2012): 298.
2. Fuhrman, Jed A., Jacob A. Cram, and David M. Needham. "Marine microbial community dynamics and their ecological interpretation." *Nature Reviews Microbiology* 13.3 (2015): 133.
3. Ward, Christopher S., et al. "Annual community patterns are driven by seasonal switching between closely related marine bacteria." *The ISME journal* 11.6 (2017): 1412
4. Barton, Andrew D., et al. "Anthropogenic climate change drives shift and shuffle in North Atlantic phytoplankton communities." *Proceedings of the National Academy of Sciences* 113.11 (2016): 2964-2969.
5. Deslippe, Julie R., et al. "Long-term warming alters the composition of Arctic soil microbial communities." *FEMS microbiology ecology* 82.2 (2012): 303-315.
6. Luo, Chengwei, et al. "Soil microbial community responses to a decade of warming as revealed by comparative metagenomics." *Appl. Environ. Microbiol.* 80.5 (2014): 1777-1786.
7. Fuhrman, Jed A., et al. "A latitudinal diversity gradient in planktonic marine bacteria." *Proceedings of the National Academy of Sciences* 105.22 (2008): 7774-7778.
8. Fierer, Noah, et al. "Microbes do not follow the elevational diversity patterns of plants and animals." *Ecology* 92.4 (2011): 797-804.
9. Abreu, Clare I., et al. "Mortality causes universal changes in microbial community composition." *Nature communications* 10.1 (2019): 2120.
10. Ratkowsky, D. A., et al. "Relationship between temperature and growth rate of bacterial cultures." *Journal of bacteriology* 149.1 (1982): 1-5.
11. Rosso, L., J. R. Lobry, and J. P. Flandrois. "An unexpected correlation between cardinal temperatures of microbial growth highlighted by a new model." *Journal of Theoretical Biology* 162.4 (1993): 447-463.
12. Friedman, Jonathan, Logan M. Higgins, and Jeff Gore. "Community structure follows simple assembly rules in microbial microcosms." *Nature Ecology & Evolution* 1.5 (2017): 0109.
13. Stubbendieck, Reed M., and Paul D. Straight. "Multifaceted interfaces of bacterial competition." *Journal of bacteriology* 198.16 (2016): 2145-2155.
14. Ratzke, Christoph, and Jeff Gore. "Modifying and reacting to the environmental pH can drive bacterial interactions." *PLoS biology* 16.3 (2018): e2004248.
15. de Carvalho, Carla CCR, and Pedro Fernandes. "Production of metabolites as bacterial responses to the marine environment." *Marine Drugs* 8.3 (2010): 705-727.
16. James, P. D. A., C. Edwards, and M. Dawson. "The effects of temperature, pH and growth rate on secondary metabolism in *Streptomyces thermoviolaceus* grown in a chemostat." *Microbiology* 137.7 (1991): 1715-1720.
17. Sun, Wei, et al. "Mechanism and effect of temperature on variations in antibiotic resistance genes during anaerobic digestion of dairy manure." *Scientific reports* 6 (2016): 30237.
18. Kim, C., and E. Ndegwa. "Influence of pH and temperature on growth characteristics of leading foodborne pathogens in a laboratory medium and select food beverages." (2018).
19. Lewington-Pearce, Leah, et al. "Temperature-dependence of minimum resource requirements alters competitive hierarchies in phytoplankton." *Oikos* (2019).
20. Hanke, Anna, et al. "Selective pressure of temperature on competition and cross-feeding within denitrifying and fermentative microbial communities." *Frontiers in Microbiology* 6 (2016): 1461.



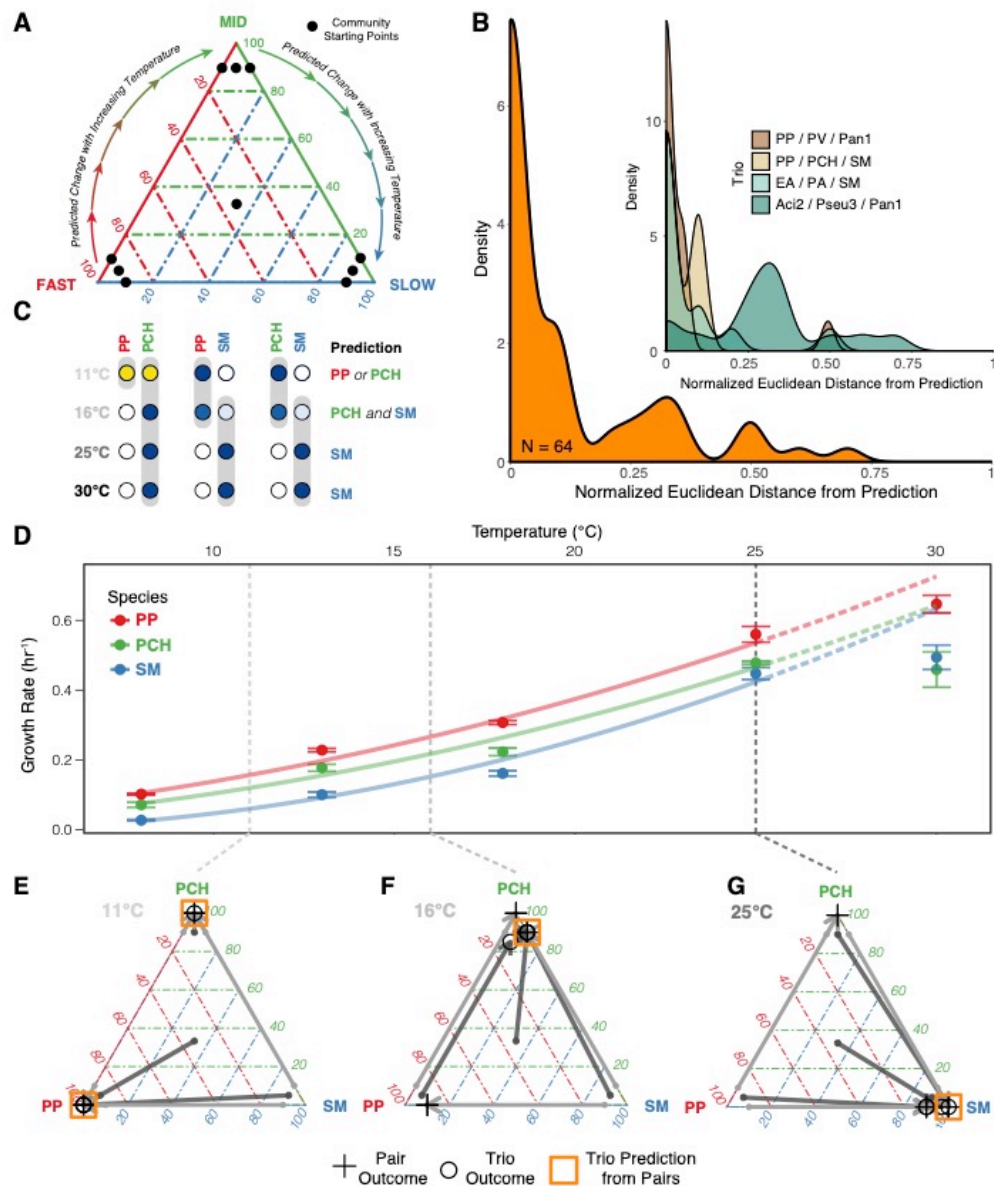
162 **Figure 1: Increasing temperature favors the slower-growing bacterial species in a coculture, despite**
163 **widening the difference in growth rates.** This figure highlights the coculture outcomes of a faster-growing
164 *Acinetobacter* species (*Aci1*) and a slower-growing *Pantoea* species (*Pan1*), both isolated from the same soil
165 sample. **(A)** *Aci1* is the faster grower regardless of temperature, and the difference in growth rates between
166 the two species accelerates as temperature increases. Increasing temperature moves the equilibrium
167 community state from competitive exclusion by *Aci1* at 16°C **(D)** to coexistence at 25°C **(E)**, and eventually to
168 *Pan1* dominance at 30°C **(F)**, with the potentially counter-intuitive result that the slower growing species is
169 favored by higher temperatures even when that change increases the gap in growth rates.



170 **Figure 2: A simple model predicts that the slower-growing species in a coculture should generically be**
 171 **favored by increasing temperature. (A)** The Lotka-Volterra competition models are parameterized by the
 172 growth rates of the two species and their competition coefficients (α), which relate between-species inhibition
 173 to within-species inhibition. A community-wide death rate (δ) can also be added to the model. **(B)** The full
 174 Lotka-Volterra competition equations, with added death rate. **(C)** With no death rate, competition outcomes
 175 are determined exclusively by the competition coefficients and do not depend on the growth rates (black
 176 points). The introduction of a death rate can alter the competitive outcome by effectively increasing the $\log(\alpha)$
 177 of the fast grower and decreasing the $\log(\alpha)$ of the slow grower by the same amount, resulting in a 45-degree
 178 movement through phase space (light gray arrows). This arrow becomes longer as the death rate increases and
 179 shorter as temperature (and accordingly growth rates) increases, implying that for a given death rate, the
 180 slower-growing species should be favored by an increase in temperature. **(D)** The growth rates of
 181 microorganisms when sufficiently below T_{Opt} are a simple function of temperature that can be modeled with
 182 two parameters: the slope of the square-root of the growth rate against temperature (b) and the minimum
 183 growth temperature (T_0).



184 **Figure 3: Theoretical predictions of which species should be favored by increasing temperature are**
185 **validated in a wide array of experimental cocultures between a diverse set of species. (A)** We tested our
186 hypothesis that the slower-growing species should be favored by increasing temperature in model two-species
187 communities drawn from 13 bacterial strains. Strains which are classified to the species level were obtained
188 from the ATCC culture collection, and strains which are classified only to the genus level were isolated from a
189 single soil sample and identified via sequencing of the 16S ribosomal subunit. Branch length of the phylogeny,
190 based on full 16S sequences, corresponds to substitutions per base pair. **(B)** We measured the growth rates
191 for each strain at a minimum of 4 temperatures in order to fit the Ratkowsky model for the range of 8°C to 25°C.
192 30°C growth rates, where the model may no longer hold, were measured directly. Line colors are matched to
193 the label color for each strain in panel **A**. **(C)** Of the 78 possible species pairs, there were 39 pairs (50%) in
194 which one strain was consistently the faster grower across the range of experimental temperatures (highlighted
195 in gray). We cocultured 38 of these pairs at 16°C, 25°C, and 30°C following the experimental protocol of Figure
196 1. We did not coculture Pan1 and Pan2 because their colony morphologies are difficult to differentiate. **(D)**
197 Heat map of coculture outcomes after a 7 day dilution cycle. Values are an average of at least 4 separate
198 cocultures comprising 3 different initial strain ratios (90% fast grower, 50% fast grower, and 10% fast grower).
199 Numbers designate species pairs as in **C**. **(E)** Boxplot of competitive outcomes at the three experimental
200 temperatures. Black lines indicate the median, lower and upper box boundaries correspond to the first and
201 third quartiles, and whiskers extend to the largest and smallest values within 1.5 times the inter-quartile range.
202 Points indicate the outcomes of individual coculture pairs, and pairs are connected by lines, which are colored
203 by the change in the mean equilibrium fast grower percentage. The two pairs in which we observe a bistable
204 outcome are not included in the plot.



205 **Figure 4: Shifts in pairwise competitive outcomes with temperature allow for prediction of the shifts**
 206 **observed in a three species community. (A)** To test the predictive accuracy of pairwise dynamics for a three
 207 species community, we determined the equilibrium outcome of each pair in the trio from 2 initial starting points
 208 and the equilibrium outcome of the full trio from four starting points. When viewed as a ternary plot with the
 209 fastest species on the bottom-left and the slowest species on the bottom-right, we predict that increasing
 210 temperature should result in a clockwise movement of the equilibrium outcome. **(B)** We calculated the
 211 Euclidean distance (normalized to the maximum possible distance) between the predicted and observed
 212 equilibrium states. The outer density plot shows the distribution of distances across all four trios, while the
 213 inner plot splits the distribution by trio. **(C)** We used the assembly rules of Friedman¹² to estimate the
 214 equilibrium community state from the pairwise dynamics of each species in the trio. In this example, the
 215 pairwise dynamics predict a bistable outcome between PP and PCH at 11°C, coexistence between PCH and
 216 SM at 16°C, and dominance by SM at 25°C and 30°C. **(D)** This figure highlights the PP/PCH/SM trio, which has
 217 a consistent growth rate hierarchy regardless of temperature. **(E-G)** The experiment validates both the
 218 predicted clockwise movement about the ternary plot and the predictive accuracy of the assembly rules. Note
 219 that the 30°C outcome is not shown because it is identical to the 25°C treatment.

MATERIALS & METHODS

SPECIES & MEDIA

220 We used two sets of bacterial species in this study: seven naturally-co-occurring taxa isolated from
221 soil and six strains ordered from the ATCC culture collection. The soil isolates were obtained by vortexing
222 a small amount of soil taken from an urban park into PBS, followed by plating onto LB agar. Colonies were
223 chosen based on the criteria that they were visually differentiable from all other strains in the study, and that
224 they were capable of growing in the defined media described below. The taxonomic identity of the soil
225 isolates was determined via sequencing of the V4-V5 16S hypervariable region, and the seven isolates were
226 found to comprise representatives from three bacterial genera: *Acinetobacter* (Aci1 and Aci2), *Pantoea* (Pan1
227 and Pan2), and *Pseudomonas* (Pseu1, Pseu2, and Pseu3). The six species obtained from ATCC were *Enterobacter*
228 *aerogenes* (EA, ATCC#13048), *Pseudomonas aurantiaca* (PA, ATCC#33663), *Pseudomonas chlororaphis* (PCH,
229 ATCC#9446), *Pseudomonas putida* (PP, ATCC#12633), *Pseudomonas veronii* (PV, ATCC#700474) and *Serratia*
230 *marcescens* (SM, ATCC#13880). All 13 strains are members of the bacterial class Gammaproteobacteria.

231 All coculture experiments in this study were carried out in S minimal medium supplemented with
232 glucose (to a concentration of 0.2%) and ammonium chloride. The medium contained 100 mM sodium
233 chloride, 5.7 mM dipotassium phosphate, 44.1 mM monopotassium phosphate, 5 mg/L cholesterol, 10 mM
234 potassium citrate pH 6 (1 mM citric acid monohydrate, 10 mM tri-potassium citrate monohydrate), 3 mM
235 calcium chloride, 3 mM magnesium sulfate, trace metals solution (0.05 mM disodium EDTA, 0.02 mM iron
236 sulfate heptahydrate, 0.01 mM manganese chloride tetrahydrate, 0.01 mM zinc sulfate heptahydrate, 0.01
237 mM copper sulfate pentahydrate), 0.93 mM ammonium chloride, and 10 mM glucose.

GROWTH RATE MODEL

238 To fit the Ratkowsky model for each strain, we calculated their growth rate at a minimum of four
239 temperatures. We used a time to threshold approach to estimate growth rates, in which monocultures with
240 known initial optical density (OD 600 nm) were spot checked every few hours. These growth rate
241 experiments were carried out as follows: frozen stocks of the desired species were streaked out on a nutrient
242 agar petri dish and, after incubation at room temperature for ~48 hours, a single colony was picked into 5
243 mL of 1X LB broth and grown overnight. 35 μ L of this LB culture was then inoculated into 5 mL of S
244 medium and grown for ~24 hours. The OD of the S medium culture was measured and the background
245 OD (measured as the OD of the same volume of sterile S medium in the same type of 96 well plate) was
246 subtracted in order to estimate population density. A \log_{10} serial dilution of the monoculture was carried out
247 on a 300 μ L 96-well plate (Falcon) so that each strain was diluted to an OD of between 10^{-1} and 10^{-6} that of
248 the overnight culture. The OD of each of these diluted cultures was checked periodically, the background
249 OD was subtracted, and the growth rate was calculated as $\log(\text{OD}_T/\text{OD}_{T=0})/T$ where $\text{OD}_{T=0}$ is the initial
250 OD of the diluted culture and OD_T is the OD at time T (measured as hours from initial time point). To
251 make sure the cultures were still in their exponential phase of growth, growth rate was only calculated for
252 measurements with $\text{OD}_T < 0.15$, and all growth rate estimates were based on a minimum of 5 measurements.
253 This method of growth rate measurement implicitly incorporates lag time, as strains with a longer lag times
254 will take longer to reach a given OD than another species with the same exponential growth rate but a
255 shorter lag time.

COCULTURE EXPERIMENTS

256 Frozen stocks of the competing species were streaked out on nutrient agar petri dishes and, after
257 incubation at room temperature for ~48 hours, a single colony of each species was picked into its own 50
258 mL Falcon tube containing 5 mL of 1X LB broth. Monocultures were grown overnight at room temperature,
259 and 35 μ L of this LB culture was then inoculated into 5 mL of S medium and grown for ~24 hours at room
260 temperature. The monocultures of each species were then OD-standardized, and the monocultures were

261 mixed together with the desired proportions. In the two species experiments, the cocultures started from
262 three initial community states: 90% fast grower / 10% slow grower, an equal split, and 10% fast grower /
263 90% slow grower. In the trio experiments, the competitions started from four initial community states: three
264 90%/5%/5% splits, each with a different species in the majority, and an even split of 33.3% of each species.
265 All competition experiments were carried out in 300 uL 96 well plates (Falcon). The initial plate was made
266 by adding 160 uL of S Media, 20 uL of 2% glucose, and 20 uL of a $1/10$ dilution of the appropriate mixed
267 cultures to each well, and was then incubated, wrapped in Parafilm and without shaking, for 24 hours at the
268 desired temperature. Each day, for seven cycles, the previous day's plate was serially diluted into new S Media
269 so that each well held 180 uL of a $1/100$ dilution of the mixed culture, and 20 uL of 2% glucose was added
270 before incubation for another 24 hours. At the end of the competition cycle, the cultures were spot plated
271 onto nutrient agar after dilution in phosphate-buffered saline, and colonies were counted by visual inspection
272 to determine the equilibrium fraction of the species.

CODE AND DATA AVAILABILITY

273 Access to the data is publicly available at <https://doi.org/10.6084/m9.figshare.8285543.v1>. All
274 code for data analysis is available from the first author by request.

ACKNOWLEDGEMENTS

275 We thank Anthony Ortiz for providing us with the bacterial soil isolates, and the members of the
276 Gore lab for their suggestions and discussion.

AUTHOR CONTRIBUTIONS

277 S.L., C.I.A., and J.G. conceived of the study. S.L. carried out the experiments with assistance from
278 C.I.A.. S.L. and C.I.A. performed the mathematical analyses. S.L. wrote the manuscript and all authors
279 edited and approved it.